Forced Intercalation Peptide Nucleic Acid Probes for the Detection of an Adenosine-to-Inosine Modification

Colin S. Swenson,[||] Hector S. Argueta-Gonzalez,[||] Sierra A. Sterling,[||] Ryan Robichaux, Steve D. Knutson, and Jennifer M. Heemstra*
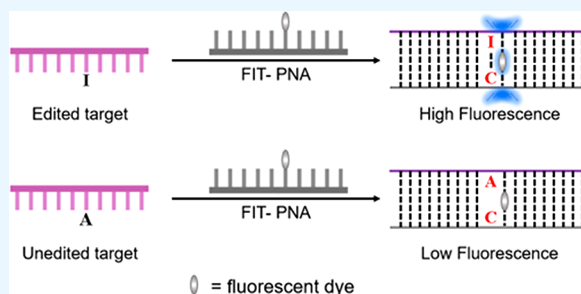
Read Online

ACCESS | Metrics & More | Article Recommendations | Supporting Information

ABSTRACT: The deamination of adenosine to inosine is an important modification in nucleic acids that functionally recodes the identity of the nucleobase to a guanosine. Current methods to analyze and detect this single nucleotide change, such as sequencing and PCR, typically require time-consuming or costly procedures. Alternatively, fluorescent "turn-on" probes that result in signal enhancement in the presence of target are useful tools for real-time detection and monitoring of nucleic acid modification. Here we describe forced-intercalation PNA (FIT-PNA) probes that are designed to bind to inosine-containing nucleic acids and use thiazole orange (TO), 4-dimethylamino-naphthalimide (4DMN), and malachite green (MG) fluorogenic dyes to detect A-to-I editing

events. We show that incorporation of the dye as a surrogate base negatively affects the duplex stability but does not abolish binding to targets. We then determined that the identity of the adjacent nucleobase and temperature affect the overall signal and fluorescence enhancement in the presence of inosine, achieving an 11-fold increase, with a limit of detection (LOD) of 30 pM. We determine that TO and 4DMN probes are viable candidates to enable selective inosine detection for biological applications.

INTRODUCTION

Genetic information is converted from DNA into proteins in a highly regulated manner using RNA as an intermediary. The posttranscriptional modification of RNA is an important cellular mechanism for regulating gene expression. In higher eukaryotes, the predominant type of RNA editing results in a change in the nucleobase identity and base pairing preference, such as the deamination of an adenosine to inosine (A → I) catalyzed by ADAR (adenosine deaminases acting on RNA) enzymes (Figure 1A).[1] The inosine base pairs with cytosine, essentially recoding an A to a G. Aberrant activity in the ADAR family has been linked to many types of cancer and neurological disorders including glioblastoma, epilepsy, and amyotrophic lateral sclerosis (ALS).[2−7] Additionally, inosine can be detected in DNA as a result of spontaneous hydrolytic or nitrosative stress induced deamination that may result in changes to downstream transcription and translation.[8]

While A → I editing is detectable by sequencing, a key challenge is the detection of single nucleotide variations in targeted transcripts. Previously our lab has developed an inosine enrichment technique for use in high-throughput RNA sequencing (RNA-seq) to identify and detect edited sites.[9] While effective, we recognized that this approach is not time- or cost-effective and is incapable of real-time analysis of RNA editing due to multistep sample preparation. As a simpler method for detecting inosine, we developed a covalent chemical labeling approach to attach reporter molecules to

edited transcripts.[10,11] However, challenges with achieving a selective reaction with inosine over other modifications such as pseudouridine made it difficult to transition this approach to live-cell and real-time applications for specific transcripts.

In addition to methods developed by the Heemstra Lab, similar work for single nucleotide polymorphism (SNP) detection includes enzyme-based approaches such as electrochemical sensing and molecular beacons. While electrochemical sensors rely on thermodynamic changes from conformational rearrangements which makes for a more sensitive system (when placed next to a mismatch), this approach can be costly in consideration of the expensive equipment required. Molecular beacons, though more cost-effective than electrochemical sensing, is a less sensitive method but requires complex designs and is prone to degradation and false signal outputs.[12]

Further studies include use of hybridization assays for detection of significant modifications in KRAS and BRAF human oncogenes. Specifically, fluorescence enhancement of intercalation probes was used to assess changes in thermal
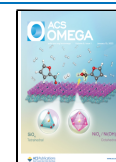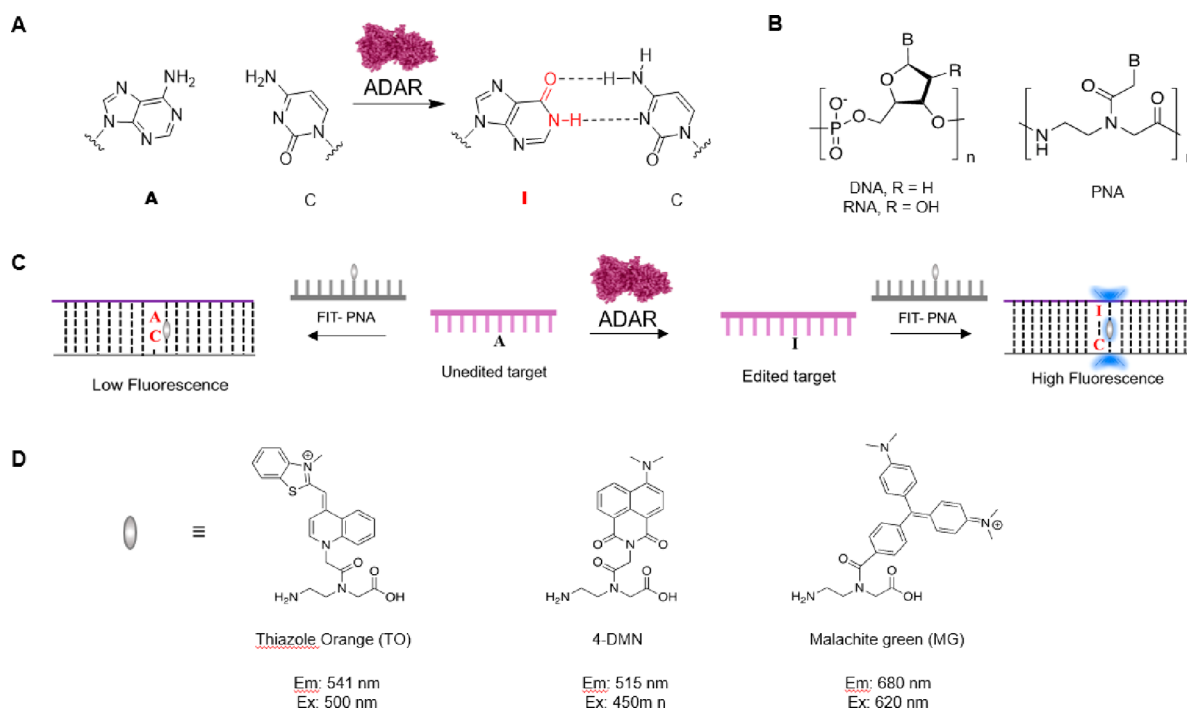
Figure 1. (A) Adenosine is deaminated to inosine by ADAR. (B) Chemical structures of DNA, RNA, and PNA. (C) PNA-FIT probes allow discrimination of edited and unedited targets by a fluorescent signal. (D) Chemical structures of fluorogenic dyes used in this study.

stability resulting from editing events and mutations.[13,14] Though these examples offer an alternative approach to detecting nucleobase changes, these methods include time-intensive experimental steps. We acknowledged the need for a method that selectively detects inosine-containing transcripts with high affinity and low background in a single step in order to overcome these limitations.

Forced intercalation (FIT) oligonucleotide probes are useful tools for detecting and imaging DNA and RNA targets *in vitro* and *in cellulo*.[12] The replacement of a canonical nucleobase with a fluorogenic dye such as thiazole orange (TO) along the backbone imparts a responsive behavior.[13,14] These probes selectively bind targets via complementary Watson−Crick−Franklin hybridization, prompting a fluorescent response from the dye and making them capable of distinguishing single mismatched nucleotides.[15] Because high affinity and specificity are requirements for performance, many research groups have turned to using peptide nucleic acid (PNA) as a convenient scaffold to design and synthesize FIT probes.
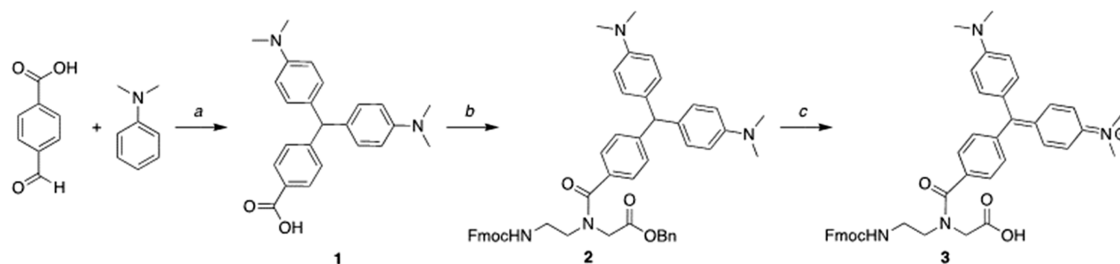
PNA is an unnatural nucleic acid mimic wherein a pseudopeptide backbone replaces the sugar phosphate backbone of canonical DNA or RNA (Figure 1B).[16] This synthetic backbone provides the molecule with stronger hybridization affinity, improved specificity, and increased resistance to enzymatic degradation, all of which are essential properties for FIT probe applications.[16−20] Therefore, it is unsurprising that many FIT-PNA probes have been developed to detect and image myriad nucleic acid targets *in vitro* and in live cells.[21−28] Kam et al. demonstrated the ability of a TO-containing FIT-PNA to image the mutated *KRAS* oncogene in live cells with single nucleotide polymorphism resolution.[29] Similarly, Seitz and co-workers exhibited the detection of a cytidine to uridine (C → U) RNA editing event using a binary probe system.[30] This was the first example of using a FIT-PNA probe to image a posttranscriptional modification expressed in live cells.

However, a FIT-PNA probe has not yet been reported to selectively target inosine-containing nucleic acids for imaging and detection of ADAR activity (Figure 1C).

Significant advances have also been made to expand the repertoire of fluorogenic dyes available for designing FIT-PNA probes.[31−36] Our group has previously experienced success using the fluorogenic dyes 4-dimethylamino-naphthalimide (4DMN) and malachite green (MG) as reporters for PNA self-assembly and protein labeling, respectively.[37,38] We hypothesized that these dyes could be incorporated into FIT-PNA probes and provide enhanced fluorescence upon binding, similar to the well characterized TO dye (Figure 1D). Here we describe the synthesis and characterization of a novel MG-containing PNA monomer followed by the design, synthesis, and characterization of FIT-PNA probes incorporating TO, 4DMN, and MG dyes to target an inosine-containing oligonucleotide. We demonstrate that the mismatched base identity and temperature effect the overall fluorescence and specificity. Through experimental observation, we conclude that TO-containing FIT-PNA probes are viable candidates for distinguishing adenosine and inosine-containing targets *in vitro* and suggest the use of triplex forming PNAs for targeting edited RNA transcripts.

RESULTS AND DISCUSSION

Design and Synthesis of Fluorogenic PNA Monomers. FIT-PNA probes utilize fluorogenic dyes that exhibit dramatic changes in fluorescence dependent upon the corresponding environment. Asymmetric cyanine-based dyes such as TO become rotationally constrained by base stacking interactions, resulting in fluorescence enhancement upon hybridization to complementary nucleic acids.[14,15,31] MG-based dyes possess a similar mechanism of fluorescence but have not yet been explored for intercalation-based signal enhancement. The relative ease of modifying the nucleobase

Scheme 1. Synthesis of MG-PNA Monomer[a]

[a](a) Zinc chloride, reflux, 52%. (b) Fmoc-(aminoethyl)glycine-benzyl-ester PNA backbone, HATU, NMM, DMF, 68%. (c) Two steps: (1) H₂, Pd/C, MeOH and (2) chloranil, MeOH, 72%.

portion of PNA has already produced many different fluorescent analogues.[14,15,31,36,37,39−44] We hypothesized that incorporating an MG base surrogate would be a simple and effective process to introduce a new class of dyes for FIT-PNA probes.

In order to synthesize an MG-containing PNA monomer (Scheme 1), we first produced the leucomalachite green carboxylic acid moiety **1** through the reaction between 4-carboxybenzaldehyde and dimethylaniline in the presence of zinc chloride. This was then coupled to an Fmoc-protected benzyl ester PNA backbone (synthesized by previously reported procedures)[45] by employing HATU and *N*-methylmorpholine to produce the protected leucomalachite green PNA monomer **2**. The benzyl group was removed by palladium catalyzed hydrogenation to afford an Fmoc-leucomalachite green PNA monomer **3**. Subsequent oxidation by choranil generated the final MG-containing PNA monomer **4**. This relatively short synthetic route afforded an MG-based PNA monomer in a simple and effective manner.

We were also curious to investigate the use of solvatochromic 4DMN dye in FIT-PNA probes, as we had previously been successful in employing this dye to signal the self-assembly and stimuli-responsive disassembly process of γ-PNA amphiphiles.[37] This dye belongs to the naphthalimide family and experiences altered emission based on an internal charge transfer mechanism that is highly dependent upon the polarity of the environment.[46] We wondered if the change in environment and solvation state between hybridized and single-stranded PNA would induce a similar change in emission intensity or wavelength and if dyes of this family could thus be useful for FIT-PNA probes. PNA monomers containing a 4DMN base surrogate were synthesized as described previously.[37]

Finally, we synthesized TO-containing PNA monomers adapted from previously reported procedures.[15,31] This well-established FIT probe dye has yet to be employed for A → I detection, and we predicted that it could be highly effective for distinguishing between edited and unedited transcripts.

Design and Synthesis of FIT-PNA Probes. In order to determine the effectiveness of TO, 4DMN, and MG dyes for detecting inosine-containing targets, we initially designed sequences complementary to a linear RNA target containing either adenosine or inosine at a defined position (Figure 2). The FIT-PNA probe was synthesized having a cytosine opposite the A/I in the RNA, as A:C mismatches are a common motif for ADAR-catalyzed editing. The dye was placed adjacent to the A:C mismatch or I:C base pair to probe the effect of simulated editing. FIT-PNA probes containing each dye at the specified position were synthesized by solid-
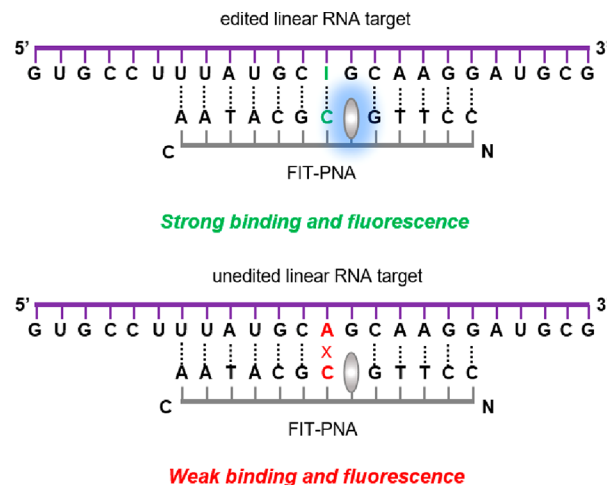

Figure 2. FIT-PNA probes hybridize to a linear RNA target and distinguish between edited and unedited targets through increased fluorescence.

phase protocols, purified by HPLC, and characterized by ESI-TOF (Table 1). The 4DMN probe was extended by two extra bases to ensure binding, as we had previously observed a large decrease in affinity when incorporating this particular dye (data not shown). Control strands complementary to the inosine-containing target were also synthesized to elucidate the change in affinity caused by including the dye.

Characterization of FIT-PNA Probes Binding to Target Transcripts. In order to characterize the change in fluorescence upon hybridization with either edited or unedited targets, we first used a linear RNA target as a proof-of-concept. Initially we confirmed binding to target RNA by thermal denaturation and determined the effect of the internal dye on the binding affinity. FIT-PNA probes were mixed with inosine-or adenosine containing RNA targets to a final concentration of 2.5 μM PNA and RNA in 1xPBS . The samples were heat denatured at 95 °C followed by annealing at 20 °C. Absorbance was monitored between 20 and 95 °C, and melting temperatures were determined in triplicate (Table 2; Figure S6). As expected, there was not a significant change in affinity between adenosine and inosine targets for fluorogenic probes. However, there were large decreases in melting temperature compared to the complementary control strands for all probes, suggesting incorporation of the dye is the major contributor to the loss in affinity. The TO-containing FIT-PNA probe displayed the least significant decrease in affinity, whereas the 4DMN and MG probes significantly perturbed the

Table 1. Sequences of FIT-PNA Probes and Confirmed Masses Determined by ESI-TOF

Probe	Sequence	Mass (M+4)$^{4+}$	Found (M+4)$^{4+}$
4DMN (15mer)	C – Lys$^+$ A A T A C G C **D** G T T C C T A – N	1070.1879	1070.6957
TO (13mer)	C – Lys$^+$ A A T A C G C **TO** G T T C C – N	947.6356	947.8971
MG (13mer)	C – Lys$^+$ A A T A C G C **MG** G T T C C – N	953.6582	953.9188
Control (15mer)	C – Lys+ A A T A C G C C G T T C C T A – N	1037.9263	1038.4390
Control (13mer)	C – Lys+ A A T A C G C C G T T C C – N	902.6226	902.8863

Table 2. UV Melting Temperatures of FIT-PNA Probes Associated with a Linear RNA Target[a]

Probe	Target	T_m (°C)	ΔT_m (°C)
4DMN (15mer)	RNA-A	54.9 ± 0.6	(-11.9)
	RNA-I	55.5 ± 0.7	(-15.1)
TO (13mer)	RNA-A	60.1 ± 0.3	(-2.4)
	RNA-I	61.6 ± 0.1	(-7.6)
MG (13mer)	RNA-A	56.7 ± 0.1	(-5.9)
	RNA-I	53.3 ± 0.2	(-15.9)
Control (15mer)	RNA-A	66.8 ± 0.5	0
	RNA-I	70.6 ± 0.4	0
Control (13mer)	RNA-A	62.5 ± 0.2	0
	RNA-I	69.1 ± 0.4	0

[a]Error is represented as SEM ($n = 3$).

duplex stability, likely due to the large increase in size as compared to native nucleobases.

After confirming the ability of fluorogenic probes to bind to the RNA targets, we characterized the fluorescence in the presence or absence of adenosine- and inosine-containing targets. FIT-PNA probes were mixed with linear RNA-A or RNA-I to a final concentration of 2.5 μM in 1xPBS. After heat denaturation and annealing, samples were incubated at room temperature for 1 h before analyzing the fluorescence. The TO probe showed a similar enhancement in fluorescence over FIT-PNA alone for both targets, whereas the 4DMN probe only displayed an appreciable fluorescence increase in the presence of the inosine target (Figure 3). However, both probes presented very little selectivity for inosine over adenosine, with the 4DMN probes and TO probes having only 2.7- and 1.2-fold increases in fluorescence, respectively. While the MG probe exhibited some enhancement in fluorescence (1.5-fold over adenosine and 5.6-fold over MG-PNA alone), the fluorescence intensity was extremely low and therefore difficult to accurately confirm the resulting activity. Thus, we decided that the MG probe was not a viable candidate for forced intercalation fluorescence enhancement and moved forward testing the 4DMN and TO probes.

To further elucidate the fluorescent properties of the FIT-PNAs, we tested the effect of the base identity opposite of the dye within the duplex. FIT probes rely upon local base stacking interactions for intercalation to adopt favorable conformations or environments for fluorescence emission.[14,15] Base stacking interactions are dependent upon the sequence and identity of local H-bonding nucleobase pairs.[47,48] We therefore hypothesized that the affinity, selectivity, and fluorescence properties may be affected by the specific target sequence and enable us to detect A-to-I editing events due to the change in base pairing and base stacking environment. We chose to employ
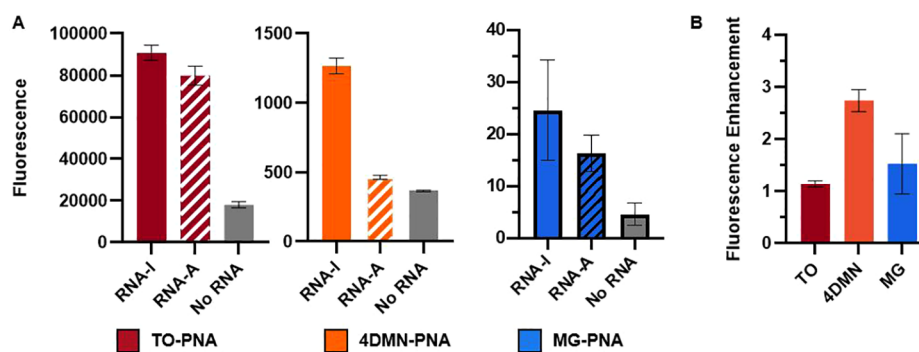

Figure 3. (A) Fluorescence of FIT-PNA probes in the presence and absence of linear RNA targets containing inosine or adenosine. Error bars represent SEM ($n = 3$). (B) Fluorescence enhancement of PNA in the presence of inosine targets compared to adenosine targets. Error bars represent SEM ($n = 3$).

DNA for these experiments as it represents a more cost-effective choice, and inosine is also found in DNA as a result of oxidative damage. We designed strands containing inosine or adenosine adjacent to each of the four canonical nucleobases: A, C, T, and G (Figure S7). TO and 4DMN FIT-PNA probes were hybridized to the DNA and fluorescence enhancement analyzed as described above. We discovered that both probes contain a preference for pairing against thymine with higher specificity for inosine over adenosine (2.9- and 2.3-fold for 4DMN and TO, respectfully) than other nucleobases (Figure 4A,B). There is not a significant preference for the other
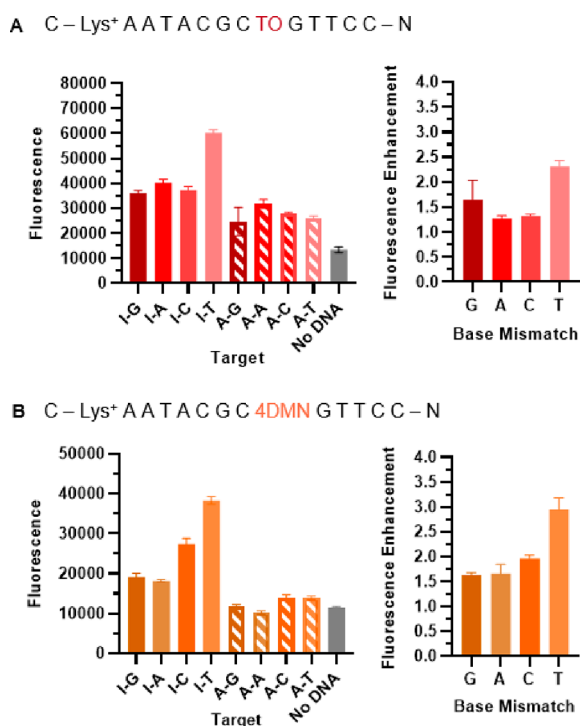

Figure 4. FIT-PNA fluorescence in the presence of DNA mismatched targets. (A) TO-PNA fluorescence and enhancement of inosine over adenosine ($n = 3$). (B) 4DMN-PNA fluorescence and enhancement of inosine over adenosine. Error bars represent SEM ($n = 3$).

nucleobases, with both probes exhibiting lower than 2-fold specificity for inosine. We then measured the effect of temperature on the fluorescence activity. By monitoring the fluorescence at temperatures from 25 to 60 °C we determined that specificity is dependent upon temperature, increasing from ~2-fold up to 11-fold for TO-PNA at 55 °C when adjacent to a thymine residue (Figure 5). The limit of detection (LOD) was calculated as 30 and 110 pM for TO and 4DMN, respectively, surpassing the LOD of 0.5, 1.8, and 14.1 nM in previously reported systems using cyanine-based ITCC, BisQ-cp, and BisQ FIT PNA probes, respectively.[33,49] For both dyes, the LOD was calculated via linear fitting, using 3 times the standard deviation of the blank sample (Figures S16 and S17). As the temperature is increased, we find that the fluorescence enhancement increases while overall fluorescence intensity decreases (Figure S8). This is not unexpected, and thus the fluorescence enhancement will be greater as the melting temperature is approached.

As the 4DMN dye substitute perturbs binding to a much greater extent than the TO substitute, there is not as significant of an effect on the fluorescence enhancement at higher

temperatures. These results indicated that TO-PNA is capable of distinguishing between inosine and adenosine containing oligonucleotides with up to an 11-fold increase in specificity at higher temperatures. We therefore moved forward designing TO probes for targeting inosine containing transcripts.

ADAR enzymes catalyze the deamination of adenosine into inosine to regulate many biological processes including gene expression and translation.[1] To date, millions of editing sites have been identified in the transcriptome with varying editing frequency at each site.[48,50] In order to validate whether a TO FIT-PNA probe can identify sites of A-to-I editing, we targeted a mimic of the HER1 RNA hairpin, a frequent and conserved editing site required for Hmg2p-induced ER remodeling (Figure 6A).[11,51] We designed and synthesized a probe complementary to the target where the PNA is capable of pairing with a majority of the loop region, which we theorized would improve strand displacement and binding (Figure 6B; SI). The fluorescence was measured in the presence and absence of HER1-I and HER1-A as described above. We observed a very slight enhancement in fluorescence in the presence of target RNA with a 1.34-fold increase in specificity for inosine over adenosine (Figure 6C). We then measured the fluorescence over a range of temperatures to see if we could improve the specificity as before. Again, we observed a decrease in fluorescence at higher temperatures; however, it was not accompanied by an increase in specificity (Figure 6D; Figure S9). Unfortunately, there was no significant effect on fluorescence enhancement with increasing temperature as had been observed with the linear targets. Due to the strong nature of the RNA hairpin, we hypothesized that the FIT-PNA probe was incapable of binding in a duplex to the targets. Using thermal denaturation, we determined that there is no significant change or additional inflection in melting temperature when the probe is introduced to the target, suggesting that the probe is not binding effectively (SI Table 1; Figure S10). The innate strong affinity of RNA hairpins makes this a difficult target for duplex forming hybridization-based probes.

In order to bind double-stranded RNA targets, researchers have developed "triplex" binding PNAs that incorporate unnatural nucleobase adducts capable of binding to the Hoogsteen face of a Watson−Crick−Franklin duplex.[52] Because adenosine deamination in mRNA occurs almost exclusively in dsRNA regions, we reasoned that this design could be particularly useful for our desired application. Recently, Sugimoto and co-workers developed a triplex-forming PNA incorporating these unnatural bases capable of recognizing and binding to an inosine-containing RNA hairpin with 100-fold greater affinity than the adenosine counterpart.[53] Using fluorophore−quencher interactions, they showed feasible competition assays for inosine detection. However, this required synthetic quencher labeled RNA and would therefore not be compatible with endogenous samples or as an imaging platform *in cellulo*. Instead, incorporating triplex-forming nucleobases into FIT-PNA probes may provide an avenue for sequence-specific inosine detection and imaging in native environments. This has been shown to be feasible in recent work by Nishizawa and co-workers, wherein including cyanine dye analogues as base surrogates in triplex forming PNAs (tFIT-PNA) resulted in increased fluorescence upon triplex formation.[54,55] We envisioned that these two approaches could be combined to create tFIT-PNA probes capable of real-time detection and imaging of inosine-containing RNA. To test this, we synthesized triplex forming
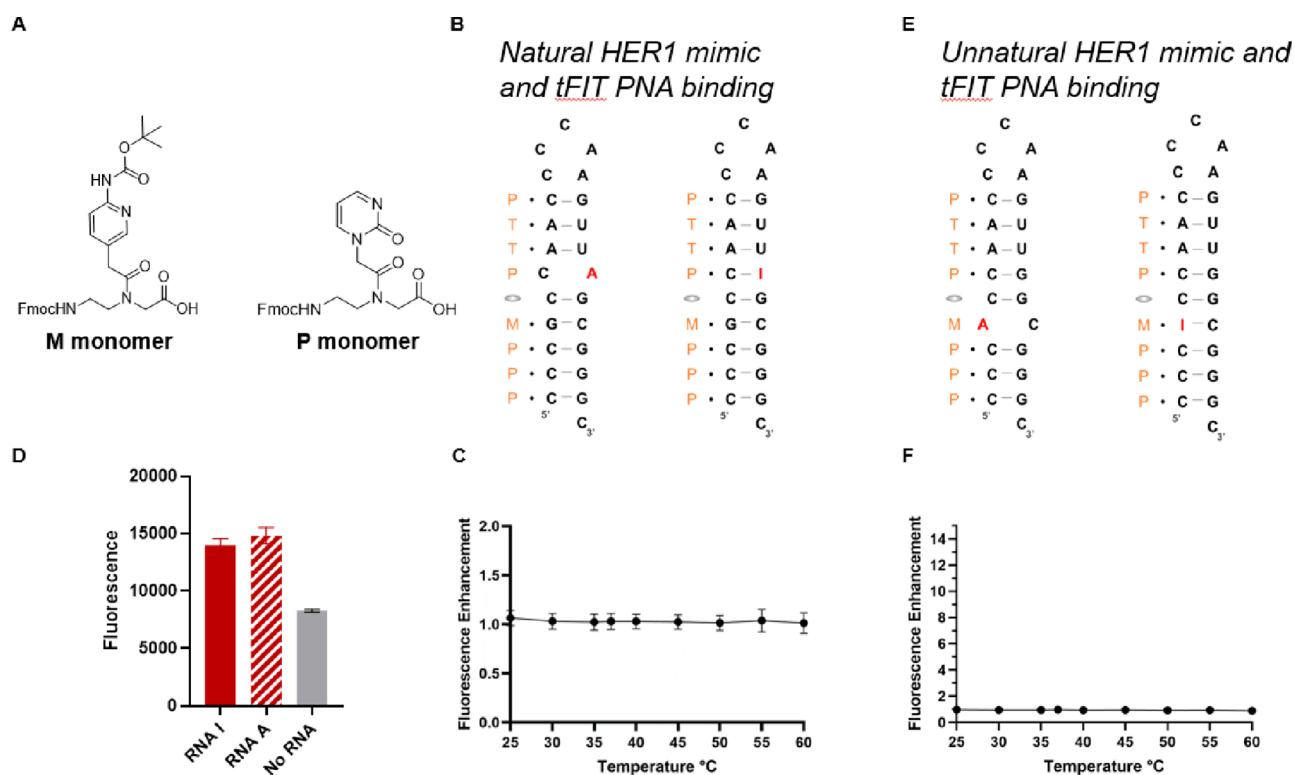
Figure 5. Effect of temperature on fluorescence enhancement and specificity of inosine over adenosine of FIT-PNA probes in the presence of mismatched DNA targets. Error bars represent SEM ($n = 3$).

Figure 6. TO FIT-PNA targeting a HER1 mimic RNA sequence. (A) Sequence of the HER1 RNA hairpin edited by ADAR. (B) Binding mode of TO FIT-PNA to the HER1-I target. (C) Fluorescence of the TO FIT-PNA probe in the presence or absence of targets. Error bars represent SEM ($n = 3$). (D) Change in fluorescence enhancement as an effect of temperature. Error bars represent SD ($n = 3$).

monomers M and P and used these to generate a triplex-forming FIT PNA probe using TO that can undergo Hoogsteen base pairing (Figure 7A), with M and P recognizing G (and likely I) and C, respectively.[56,57] Initially, the tFIT-PNA probe was designed to be complementary to the 5′-HER1 hairpin sequence, complementary to the site of interest (Figure 7B).

Upon synthesis and characterization (Figure S15), the probe was tested for target-specific fluorescence enhancement. However, while we observed increased fluorescence compared to the no target control, there was no specificity displayed for

inosine over adenosine (Figure 7D). We then tested fluorescence enhancement over a range of temperatures (Figure 7E), but unlike our FIT probes binding single-stranded oligonucleotides, in this case we did not see an increase in selectivity. Finally, to further test our probe, we completed a preliminary, single replicate study on an unnatural variant of HER1, positioning the A-to-I edit closer in proximity to the TO tFIT PNA probe (Figure 7C). However, this did not result in a significant change in specificity for detecting inosine over adenosine (Figure 7F). These results were surprising given the previous success of tFIT probes. While

Figure 7. TO tFIT-PNA targeting a natural and unnatural HER1 mimic RNA sequence. (A) Chemical structure of M and P PNA monomers. (B) Binding mode of TO tFIT-PNA to the natural HER1-I targets. (C) Binding mode of TO tFIT-PNA to the unnatural HER1-I targets (D) . Fluorescence of the TO FIT-PNA probe in the presence or absence of targets. Error bars represent SEM ($n = 3$). (E) Change in the fluorescence enhancement as a function of temperature. Error bars represent SD ($n = 3$). (F) Change in fluorescence enhancement as a function of temperature.

we did not ultimately achieve our desired outcome of using these probes to detect inosine in dsRNA regions, we felt that reporting these negative results was important for advancing discussion of the design of tFIT probes and could be of value to the scientific community.

CONCLUSIONS

The deamination of adenosine to inosine is an important modification in nucleic acids used to regulate numerous cellular functions. Distinguishing this single nucleotide change in a sequence specific manner in real-time remains a challenge. We explored the use of FIT-PNA probes for inosine detection by evaluating three different fluorogenic dyes: thiazole orange, 4-dimethylamino-naphthalimide, and malachite green. PNA monomers containing each dye as a base surrogate were synthesized and incorporated into oligomers complementary to an inosine-containing target of interest. Thermal melting studies revealed that the negative contribution on stability from the dye was greater than the mismatch resulting from A-to-I editing. Fluorescence studies showed that both TO and 4DMN resulted in an increased signal in the presence of RNA and that each dye contained a preference for an adjacent thymine residue in DNA. Greater selectivity for inosine over adenosine in DNA followed increasing temperature up to 11-fold for TO when paired against a thymine base. Unfortunately, the FIT-PNA probes were incapable of disrupting innately strong RNA duplex regions typically found near edited sites. We sought to overcome this challenge using a triplex forming the PNA probe. While the triplex was capable of forming and demonstrated an initial fluorescence increase upon binding to hairpin RNA, it did not show nucleotide-level

specificity; thus, the TO tFIT-PNA probe is not capable of detecting inosine over adenosine in the context tested. Together, the data presented demonstrate the ability of TO- and 4DMN-containing FIT-PNA probes to distinguish between inosine and adenosine-containing nucleic acids, particularly in DNA. We anticipate that further exploration of dye identity, target selectivity, and sequence design will make these probes useful for a range of inosine detection platforms, including live-cell imaging and real-time enzyme activity monitoring

MATERIALS AND METHODS

Abbreviations are as follows: Fmoc, fluorenylmethyloxycarbonyl; DMF, dimethylformamide; HATU, 1-[Bis-(dimethylamino)methylene]-1H-1,2,3-triazolo[4,5-b]-pyridinium 3-oxid hexafluorophosphate; NMM, N-methylmorpholine; DIPEA, diisopropylethylamine; TFA, trifluoroacetic acid; DCM, dichloromethane; Boc, *tert*-butyloxycarbonyl; NMP, N-methyl-2-pyrrolidone; PyBOP, benzotriazol-1-yl-oxy-tripyrrolidinophosphonium hexafluorophosphate; FCC, flash column chromatography.

Synthesis of Fluorogenic PNA Monomers. Canonical PNA monomers of A, C, T, and G were purchased from PolyOrg, Inc. All other reagents and solvents were acquired from Chem-Impex, Millipore Sigma, or Fisher Scientific and used without further purification unless otherwise stated. All reactions were performed under inert nitrogen gas using dry solvents unless otherwise stated. Dry solvents were dispensed from a J. C. Meyer solvent system prior to use to ensure dryness. Product formation was monitored by thin layer chromatography (TLC) on Merck silica gel 60 F254 glass

plates and visualized using UV light and staining with ninhydrin or potassium permanganate followed by heating. Flash column chromatography was performed under pressurized air using SiliaFlash F60 grade silica acquired from SiliCycle, Inc. Final products were confirmed and characterized by proton and carbon nuclear magnetic resonance (NMR) using a Varian Inova 400 MHz spectrometer. Spectra were analyzed using the MestReNova software. An Agilent 6230 electrospray ionization time-of-flight (ESI-TOF) mass spectrometer confirmed the mass of products. The (aminoethyl)-glycine benzyl ester PNA backbone, thiazole orange, 4DMN, P, and M monomers were synthesized by previously reported procedures.[15,31,37,45,56,57]

p-Carboxyl Leucomalachite Green (1). To a 100 mL round-bottom flask was added 4-carboxybenzaldehyde (96.3 mmol), *N*,*N*-dimethylaniline (6.65 mmol), and zinc chloride (13.4 mmol). The mixture was refluxed for 5 h, after which TLC showed complete consumption of the starting material. The reaction was cooled to room temperature, filtered, and concentrated under reduced pressure. The crude mixture was recrystallized in methanol to yield the purified product as a light blue solid (3.47 mmol, 52% yield). ^{1}H NMR (400 MHz, DMSO-d_6) δ 12.23 (s, 1H), 7.83 (d, 2H), 7.15 (d, 2H), 6.83 (d, 4H), 6.64 (d, 4H), 5.38 (s, 1H) 2.84 (s, 12H). ^{13}C NMR (400 MHz, DMSO-d_6) δ 148.84, 131.60, 129.41, 129.26, 128.83, 112.41, 109.58, 54.11, 40.24. HRMS (ESI-TOF) m/z 375.1995 (calcd [M + H]$^+$ = 375.1994).

Fmoc Leucomalachite Green (Aminoethyl)glycine Benzyl Ester (2). Compound **1** (1.52 mmol) was dissolved in DMF (6 mL) in a 100 mL round-bottom flask. HATU (2.41 mmol) was added followed by NMM (3.63 mmol), and the reaction was stirred for 30 min. Fmoc benzyl ester PNA backbone (1.21 mmol) dissolved in DMF (2 mL) and 1 equiv of NMM was added to the reaction and stirred overnight at RT after which full consumption of backbone was indicated by TLC. The reaction was concentrated under reduced pressure and purified by FCC using a gradient of hexane to ethyl acetate to yield the final product as a light blue solid (0.82 mmol, 68% yield). ^{1}H NMR (400 MHz, DMSO-d_6, two rotamers) δ 7.86 (d, 2H), 7.65 and 7.59 (d, 2H minor and major rotamer), 7.40−7.36 (m, 6H), 7.29−7.25 (m, 4H), 7.17 (d, 2H), 7.03 and 6.99 (d, 2H, minor and major rotamer), 6.96 and 6.83 (d, 4H, minor and major rotamer), 6.63 and 6.58 (d, 4H, minor and major rotamer), 5.33 and 5.27 (s, 1H, minor and major rotamer), 5.18 (s, 2H), 4.24 (s, 2H), 4.20 (t, 1H), 4.16 (s, 2H), 3.50; 3.25 (m, 2H), 3.12−3.07 (m, 2H), 2.84 and 2.81 (s, 12H, minor and major rotamer). ^{13}C NMR (400 MHz, DMSO-d_6) δ 171.46, 169.16, 155.92, 148.78, 143.86, 140.74, 135.87, 133.08, 131.79, 129.40, 128.71, 128.45, 128.11, 127.94, 127.61, 127.02, 126.51, 126.26, 125.07, 120.11, 112.34, 65.98, 65.48, 59.76, 53.97, 46.73, 40.23, 20.77, 14.09. HRMS (ESI-TOF) m/z 787.4603 (calcd [M + H]$^+$ = 787.3781).

Fmoc Malachite Green PNA Monomer (3). Compound **2** (0.132 mmol) was dissolved in methanol (2.5 mL) under nitrogen gas. Palladium on activated carbon (∼10%/wt equiv) was added, and the nitrogen was replaced with a balloon of hydrogen gas. The reaction was stirred overnight, after which TLC indicated full consumption of the starting material. The reaction was filtered through Celite and concentrated under reduced pressure. To the crude material dissolved in methanol (2 mL) was added chloranil (0.866 mmol). The reaction was stirred overnight and concentrated under reduced pressure. The product was purified by FCC using a gradient of DCM to

15% methanol in DCM to yield the purified monomer as a dark blue solid (0.107 mmol, 72% yield). ^{1}H NMR (600 MHz, DMSO-d_6) δ 12.7 (s, 1H), 7.87−7.84 (m, 2H), 7.67−7.63 (m, 2H), 7.57 (d, 2H), 7.38 (t, 2H), 7.35 (t, 1H), 7.27(t, 2H), 7.23−7.18 (m, 4H), 6.94 (d, 2H), 6.62 (d, 2H), 6.57 (d, 2H), 4.30 (d, 1H), 4.18 (t, 2H), 4.09 (s, 2H), 3.48; 3.39 (m, 2H), 3.11−3.07 (m, 2H), 2.86 (s, 6H), 2.62 (s, 6H). ^{13}C NMR (400 MHz, DMSO-d_6) δ 171.34, 170.69, 155.88, 150.06, 148.96, 143.83, 140.71, 135.94, 135.80, 133.67, 129.38, 128.53, 128.43, 127.58, 127.49, 127.00, 125.62, 125.33, 125.02, 120.08, 113.99, 111.34, 79.83, 65.45, 46.63, 40.49, 40.16, 40.06, 38.25. HRMS (ESI-TOF) m/z 695.3150 (calcd [M]$^+$ = 695.3228).

Synthesis of FIT-PNA Probes. PNA oligomers were synthesized on a Biotage SP Wave semiautomatic peptide synthesizer under microwave assistance. Synthesis began by downloading 50 mg of a rink amide MBHA (0.52 mmol/g) with 10 μmol of Fmoc-Lys(Boc)-OH using HATU (1.5 equiv), DIPEA (1.5 equiv), and 2,6-lutidine (1.5 equiv) in 200 μL of dry NMP for 1 h at room temperature. The resin was then capped using a solution of 9% acetic anhydride and 13% 2,6-lutidine in DMF. The resin was washed (5 × 1 mL DMF, 5 × 1 mL DCM, 3 × 1 mL DMF) and deprotected using 25% piperidine in DMF (3 × 1 mL for 2 min). Successive couplings were performed by first mixing Fmoc PNA monomer (5 equiv) with HATU (5 equiv), DIPEA (5 equiv), and 2,6-lutidine (5 equiv) in 300 μL of dry NMP and preactivating for 10 min. The activated solution was then added to the resin, and coupling proceeded using microwave assistance at 75 °C for 6 min. The resin was then washed (5 × 1 mL DMF), capped using a capping solution (2 × 1 mL for 5 min), washed (5 × 1 mL DMF, 5 × 1 mL DCM, 3 × 1 mL DMF), and deprotected using deprotection solution (3 × 1 mL for 2 min). A final washing step (5 × 1 mL DMF, 5 × 1 mL DCM, 3 × 1 mL DMF) completed a coupling cycle. For the thiazole orange PNA monomer, HATU was replaced with PyBOP (5 equiv) for activation and coupling steps, which improved solubility and efficiency. Loading and monomer coupling efficiency was monitored by absorbance at 301 nm of the dibenzofulvene−piperidine adduct using a Nanodrop 2000 spectrophotometer. Upon completion of synthesis, the resin was washed with DCM (3 × 1 mL) and dried under vacuum to prepare for cleavage. Cleavage from the resin was performed three times using 500 μL of a solution of 95% TFA, 2.5% H$_2$O, and 2.5% triisopropylsilane for 1 h. The crude oligomer was precipitated by addition of ether and centrifuged to a pellet. The pellet was washed with ether (3×) and dissolved in 50% acetonitrile in H$_2$O for purification. The crude oligomer was purified by reverse-phase HPLC using an Agilent Eclipse XDB-C18 5 μm, 9.4 × 250 mm column at 60 °C with a flow rate of 2 mL/min, monitored at 260 nm using a 15 min linear gradient (10−40%) of 0.1% TFA/acetonitrile in 0.1% TFA/water. FIT-PNA probes containing 4DMN were also monitored at 420 nm, while thiazole orange and malachite green were monitored at 510 and 620 nm, respectively. Identity and retention time were confirmed by ESI-TOF mass spectrometry.

Melting Temperature Analysis of FIT-PNA Probes with RNA and DNA. Samples of the FIT-PNA probe and RNA or DNA at 2.5 μM in 1xPBS were prepared from stock solutions and annealed by heating to 95 °C for 5 min, followed by incubation at 20 °C for 1 h. A 150 μL volume of each sample was transferred to an 8-cell quartz microcuvette with a 1 cm path length. Absorbance was monitored at 260 nm from 20 to 95 °C at a rate of 0.5 °C/min using a Shimadzu UV-1800

spectrophotometer equipped with a temperature controller and Julabo CORIO CD water circulator. Melting temperatures were determined by the first derivate method using a total of three independent trials. Molar absorptivity values at 260 nm for the dye-containing PNA monomers are as follows: 4DMN = 8507 $M^{-1}cm^{-1}$; TO = 6600 $M^{-1}cm^{-1}$; MG = 4900 $M^{-1}cm^{-1}$.

Fluorescence Enhancement of FIT-PNA Probes. Samples were prepared in triplicate from stock solutions in 1xPBS composed of 2.5 μM FIT-PNA probe alone, 2.5 μM FIT-PNA with 2.5 μM inosine-containing RNA or DNA target, 2.5 μM FIT-PNA probe with 2.5 μM adenosine-containing RNA or DNA target, and a 1xPBS blank. The samples were heated to 95 °C for 5 min followed by incubation at room temperature for 1 h for annealing. A 60 μL volume of each sample was transferred to a 384 microwell plate and covered with a clear lid. Fluorescence was measured using a Biotek Cytation 5 Plate Reader (excitation/emission = 450/515 nm for 4DMN; 500/541 nm for TO; 620/680 nm for MG). Fluorescence spectra were also measured for each probe (excitation/emission = 450/480−700 nm for 4DMN; 500/532−700 nm for TO). Fluorescence enhancement for inosine over adenosine was determined by dividing the fluorescence values from samples with inosine-containing targets by samples with adenosine-containing targets. Fluorescence enhancement over the background was determined by dividing the fluorescence values by that of the sample composed of FIT-PNA probe alone. Values were calculated using a total of three independent trials.

Thermal Evaluation of Fluorescence Enhancement of FIT-PNA Probes. Samples prepared from determining fluorescence enhancement were used to elucidate the effect of temperature on fluorescence. Samples were placed in a 384 microwell plate and fluorescence was measured every 5 °C from 25 to 60 °C, including a reading at 37 °C (excitation/ emission = 450/515 nm for 4DMN; 500/541 nm for TO; 620/680 nm for MG) using a Biotek Cytation 5 Plate Reader. Fluorescence enhancement at each temperature was determined as previously described. Values were calculated using a total of three independent trials.

ASSOCIATED CONTENT

Ⓢ Supporting Information

The Supporting Information is available free of charge at https://pubs.acs.org/doi/10.1021/acsomega.2c03568.

Figures, tables, and characterization of fluorogenic monomers and FIT-PNA probes (PDF)

AUTHOR INFORMATION

Corresponding Author

Jennifer M. Heemstra − *Department of Chemistry, Emory University, Atlanta, Georgia 30322, United States; Department of Chemistry, Washington University, St. Louis, Missouri 63130, United States;* ⓞ orcid.org/0000-0002-7691-8526; Email: heemstra@wustl.edu

Authors

Colin S. Swenson − *Department of Chemistry, Emory University, Atlanta, Georgia 30322, United States;* ⓞ orcid.org/0000-0002-4883-8684

Hector S. Argueta-Gonzalez − *Department of Chemistry, Emory University, Atlanta, Georgia 30322, United States*

Sierra A. Sterling − *Department of Chemistry, Emory University, Atlanta, Georgia 30322, United States;* ⓞ orcid.org/0000-0002-0023-8487

Ryan Robichaux − *Department of Chemistry, Emory University, Atlanta, Georgia 30322, United States*

Steve D. Knutson − *Department of Chemistry, Emory University, Atlanta, Georgia 30322, United States;* ⓞ orcid.org/0000-0001-6822-464X

Complete contact information is available at: https://pubs.acs.org/10.1021/acsomega.2c03568

REFERENCES

(1) Meier, J. C.; Kankowski, S.; Krestel, H.; Hetsch, F. RNA editing—systemic relevance and clue to disease mechanisms? *Front. Mol. Neurosci.* **2016**, DOI: 10.3389/fnmol.2016.00124.

(2) Maas, S.; Patt, S.; Schrey, M.; Rich, A. Underediting of glutamate receptor GluR-B mRNA in malignant gliomas. *Proc. Natl. Acad. Sci. U. S. A.* **2001**, *98*, 14687−14692.

(3) Chen, L.; et al. Recoding RNA editing of AZIN1 predisposes to hepatocellular carcinoma. *Nat. Med.* **2013**, *19*, 209−216.

(4) Brusa, R.; et al. Early-onset epilepsy and postnatal lethality associated with an editing-deficient GluR-B allele in mice. *Science* **1995**, *270*, 1677−1680.

(5) Krestel, H. E.; et al. A genetic switch for epilepsy in adult mice. *J. Nanoneurosci.* **2004**, *24*, 10568−10578.

(6) Kwak, S.; Kawahara, Y. Deficient RNA editing of GluR2 and neuronal death in amyotropic lateral sclerosis. *J. Mol. Med. (Berl).* **2005**, *83*, 110−120.

(7) Kawahara, Y.; et al. RNA editing and death of motor neurons. *Nature* **2004**, *427*, 801−801.

(8) Alseth, I.; Dalhus, B.; Bjørås, M. Inosine in DNA and RNA. *Curr. Opin. Genet. Dev.* **2014**, *26*, 116−123.

(9) Knutson, S. D.; Arthur, R. A.; Johnston, H. R.; Heemstra, J. M. Selective enrichment of A-to-I edited transcripts from cellular RNA using endonuclease V. *J. Am. Chem. Soc.* **2020**, *142*, 5241−5251.

(10) Knutson, S. D.; Ayele, T. M.; Heemstra, J. M. Chemical labeling and affinity capture of inosine-containing RNAs using acrylamido-fluorescein. *Bioconjugate Chem.* **2018**, *29*, 2899−2903.

(11) Knutson, S. D.; et al. Chemical Profiling of A-to-I RNA Editing Using a Click-Compatible Phenylacrylamide. *Chem. - Eur. J.* **2020**, *26*, 9874−9878.

(12) Tomoike, F.; Abe, H. RNA imaging by chemical probes. *Adv. Drug Delivery Rev.* **2019**, *147*, 44−58.

(13) Seitz, O.; Bergmann, F.; Heindl, D. A Convergent Strategy for the Modification of Peptide Nucleic Acids: Novel Mismatch-Specific PNA-Hybridization Probes. *Angew. Chem., Int. Ed.* **1999**, *38*, 2203−2206.

(14) Köhler, O.; Seitz, O. Thiazole orange as fluorescent universal base in peptide nucleic acids. *Chem. Commun. (Cambridge, U. K.)* **2003**, 2938−2939.

(15) Köhler, O.; Jarikote, D. V.; Seitz, O. Forced intercalation probes (FIT Probes): thiazole orange as a fluorescent base in peptide nucleic acids for homogeneous single-nucleotide-polymorphism detection. *ChemBioChem.* **2005**, *6*, 69−77.

(16) Nielsen, P.; Egholm, M.; Berg, R.; Buchardt, O. Sequence-selective recognition of DNA by strand displacement with s thymine—snbstimted poly amide. *Science* **1991**, *254*, 1497−1500.

(17) Demidov, V. V.; et al. Stability of peptide nucleic acids in human serum and cellular extracts. *Biochemical pharmacology* **1994**, *48*, 1310−1313.

(18) Egholm, M.; et al. PNA hybridizes to complementary oligonucleotides obeying the Watson−Crick hydrogen-bonding rules. *Nature* **1993**, *365*, 566−568.

(19) Uhlmann, E.; Peyman, A.; Breipohl, G.; Will, D. W. PNA: synthetic polyamide nucleic acids with unusual binding properties. *Angew. Chem., Int. Ed.* **1998**, *37*, 2796−2823.

(20) Nielsen, P. E.; Egholm, M.; Buchardt, O. Peptide nucleic acid (PNA). A DNA mimic with a peptide backbone. *Bioconjugate Chem.* **1994**, *5*, 3−7.

(21) Kam, Y.; et al. Detection of a long non-coding RNA (CCAT1) in living cells and human adenocarcinoma of colon tissues using FIT−PNA molecular beacons. *Cancer Lett. (N. Y., NY, U. S.)* **2014**, *352*, 90−96.

(22) Torres, A. G.; et al. Chemical structure requirements and cellular targeting of microRNA-122 by peptide nucleic acids anti-miRs. *Nucleic Acids Res.* **2012**, *40*, 2152−2167.

(23) Kummer, S.; et al. Fluorescence imaging of influenza H1N1 mRNA in living infected cells using single-chromophore FIT-PNA. *Angew. Chem., Int. Ed.* **2011**, *50*, 1931−1934.

(24) Kummer, S.; et al. PNA FIT-probes for the dual color imaging of two viral mRNA targets in influenza H1N1 infected live cells. *Bioconjugate Chem.* **2012**, *23*, 2051−2060.

(25) Tonelli, A.; et al. Real time RNA transcription monitoring by Thiazole Orange (TO)-conjugated Peptide Nucleic Acid (PNA) probes: norovirus detection. *Molecular BioSystems* **2011**, *7*, 1684−1692.

(26) Sonar, M. V.; et al. Fluorescence detection of KRAS2 mRNA hybridization in lung cancer cells with PNA-peptides containing an internal thiazole orange. *Bioconjugate Chem.* **2014**, *25*, 1697−1708.

(27) Socher, E.; et al. FIT probes: peptide nucleic acid probes with a fluorescent base surrogate enable real-time DNA quantification and single nucleotide polymorphism discovery. *Anal. Biochem.* **2008**, *375*, 318−330.

(28) Hashoul, D.; et al. Red-emitting FIT-PNAs:"On site" detection of RNA biomarkers in fresh human cancer tissues. *Biosens. Bioelectron.* **2019**, *137*, 271−278.

(29) Kam, Y.; Rubinstein, A.; Nissan, A.; Halle, D.; Yavin, E. Detection of endogenous K-ras mRNA in living cells at a single base resolution by a PNA molecular beacon. *Mol. Pharmaceutics* **2012**, *9*, 685−693.

(30) Fang, G.-m.; et al. A bright FIT-PNA hybridization probe for the hybridization state specific analysis of a C→ U RNA edit via FRET in a binary system. *Chem. Sci.* **2018**, *9*, 4794−4800.

(31) Bethge, L.; Jarikote, D. V.; Seitz, O. New cyanine dyes as base surrogates in PNA: Forced intercalation probes (FIT-probes) for homogeneous SNP detection. *Bioorg. Med. Chem.* **2008**, *16*, 114−125.

(32) Kolevzon, N.; Hashoul, D.; Naik, S.; Rubinstein, A.; Yavin, E. Single point mutation detection in living cancer cells by far-red emitting PNA−FIT probes. *Chem. Commun. (Cambridge, U. K.)* **2016**, *52*, 2405−2407.

(33) Socher, E.; Knoll, A.; Seitz, O. Dual fluorophore PNA FIT-probes− extremely responsive and bright hybridization probes for the sensitive detection of DNA and RNA. *Org. Biomol. Chem.* **2012**, *10*, 7363−7371.

(34) Tedeschi, T.; Tonelli, A.; Sforza, S.; Corradini, R.; Marchelli, R. A pyrenyl-PNA probe for DNA and RNA recognition: Fluorescence and UV absorption studies. *Artificial DNA: PNA & XNA* **2010**, *1*, 83−89.

(35) Mansawat, W.; Boonlua, C.; Siriwong, K.; Vilaivan, T. Clicked polycyclic aromatic hydrocarbon as a hybridization-responsive fluorescent artificial nucleobase in pyrrolidinyl peptide nucleic acids. *Tetrahedron* **2012**, *68*, 3988−3995.

(36) Okamoto, A.; Tanabe, K.; Saito, I. Synthesis and properties of peptide nucleic acids containing a psoralen unit. *Org. Lett.* **2001**, *3*, 925−927.

(37) Swenson, C. S.; Velusamy, A.; Argueta-Gonzalez, H. S.; Heemstra, J. M. Bilingual peptide nucleic acids: encoding the languages of nucleic acids and proteins in a single self-assembling biopolymer. *J. Am. Chem. Soc.* **2019**, *141*, 19038−19047.

(38) Ayele, T. M.; Knutson, S. D.; Ellipilli, S.; Hwang, H.; Heemstra, J. M. Fluorogenic photoaffinity labeling of proteins in living cells. *Bioconjugate Chem.* **2019**, *30*, 1309−1313.

(39) Gangamani, B. P.; Kumar, V. A. 2-Aminopurine peptide nucleic acids (2-ap PNA): intrinsic fluorescent PNA analogues for probing PNA−DNA interaction dynamics. *Chem. Commun. (Cambridge, U. K.)* **1997**, 1913−1914.

(40) Ikeda, H.; Yoshida, K.; Ozeki, M.; Saito, I. Synthesis and characterization of flavin-tethered peptide nucleic acid. *Tetrahedron Lett.* **2001**, *42*, 2529−2531.

(41) Cichon, M. K.; Haas, C. H.; Grolle, F.; Mees, A.; Carell, T. Efficient interstrand excess electron transfer in PNA: DNA hybrids. *J. Am. Chem. Soc.* **2002**, *124*, 13984−13985.

(42) Wilhelmsson, L. M.; Holmén, A.; Lincoln, P.; Nielsen, P. E.; Nordén, B. A highly fluorescent DNA base analogue that forms watson− crick base pairs with guanine. *J. Am. Chem. Soc.* **2001**, *123*, 2434−2435.

(43) Ikeda, H.; Nakamura, Y.; Saito, I. Synthesis and characterization of naphthalimide-containing peptide nucleic acid. *Tetrahedron Lett.* **2002**, *43*, 5525−5528.

(44) Okamoto, A.; Tainaka, K.; Saito, I. Clear distinction of purine bases on the complementary strand by a fluorescence change of a novel fluorescent nucleoside. *J. Am. Chem. Soc.* **2003**, *125*, 4972−4973.

(45) Feagin, T. A.; Shah, N. I.; Heemstra, J. M. Convenient and scalable synthesis of Fmoc-protected peptide nucleic acid backbone. *J. Nucleic Acids.* **2012**, *2012*, 354549.

(46) Zhang, W.; Wang, Y.; Xu, Y.; Qian, X. New fluorescent conjugates of uridine nucleoside and substituted 1, 8-naphthalimide: synthesis, weak interactions and solvent effects on spectra. *Monatsh. Chem.* **2003**, *134*, 393−402.

(47) Riley, K. E.; Hobza, P. On the importance and origin of aromatic interactions in chemistry and biodisciplines. *Acc. Chem. Res.* **2013**, *46*, 927−936.

(48) Karabıyık, H.; Sevinçek, R.; Karabıyık, H. *π*-Cooperativity effect on the base stacking interactions in DNA: is there a novel stabilization factor coupled with base pairing H-bonds? *Phys. Chem. Chem. Phys.* **2014**, *16*, 15527−15538.

(49) Tepper, O.; Zheng, H.; Appella, D. H.; Yavin, E. Cyclopentane FIT-PNAs: bright RNA sensors. *Chem. Commun. (Cambridge, U. K.)* **2021**, *57*, 540−543.

(50) Ramaswami, G.; Li, J. B. RADAR: a rigorously annotated database of A-to-I RNA editing. *Nucleic Acids Res.* **2014**, *42*, D109−D113.

(51) Wang, Y.; Park, S.; Beal, P. A. Selective recognition of RNA substrates by ADAR deaminase domains. *Biochemistry* **2018**, *57*, 1640−1651.

(52) Zengeya, T.; Gupta, P.; Rozners, E. Triple-helical recognition of RNA using 2-aminopyridine-modified PNA at physiologically relevant conditions. *Angew. Chem.* **2012**, *124*, 12761−12764.

(53) Annoni, C.; Endoh, T.; Hnedzko, D.; Rozners, E.; Sugimoto, N. Triplex-forming peptide nucleic acid modified with 2-aminopyridine as a new tool for detection of A-to-I editing. *Chem. Commun. (Cambridge, U. K.)* **2016**, *52*, 7935−7938.

(54) Sato, T.; Sato, Y.; Nishizawa, S. Triplex-forming peptide nucleic acid probe having thiazole orange as a base surrogate for fluorescence sensing of double-stranded RNA. *J. Am. Chem. Soc.* **2016**, *138*, 9397−9400.

(55) Chiba, T.; Sato, T.; Sato, Y.; Nishizawa, S. Red-emissive triplex-forming PNA probes carrying cyanine base surrogates for fluorescence sensing of double-stranded RNA. *Org. Biomol. Chem.* **2017**, *15*, 7765−7769.

(56) Hnedzko, D.; Cheruiyot, S. K.; Rozners, E. Using Triple-Helix-Forming Peptide Nucleic Acids for Sequence-Selective Recognition of Double-Stranded RNA. *Curr. Protoc. Nucleic Acid Chem.* **2014**, *58*, 4.60.61−64.60.23.

(57) Kumpina, I.; et al. Synthesis and RNA-binding properties of extended nucleobases for triplex-forming peptide nucleic acids. *Journal of Organic Chemistry* **2019**, *84*, 13276−13298.